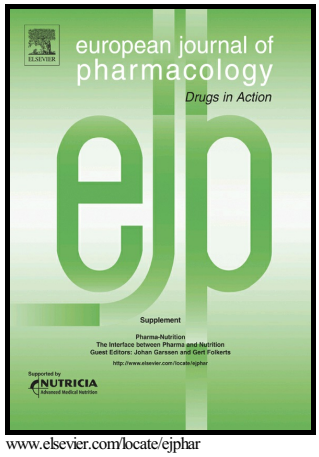

www.elsevier.com/locate/ejphar

Magnesium lithospermate B prevents phenotypic transformation of pulmonary arteries in rats with hypoxic pulmonary hypertension through suppression of NADPH oxidase

Tao Li, Xiu-Ju Luo, E-Li Wang, Nian-Sheng Li, Xiao-Jie Zhang, Feng-Lin Song, Jin-Fu Yang, Bin Liu, Jun Peng

PII: S0014-2999(19)30028-7
DOI: https://doi.org/10.1016/j.ejphar.2019.01.020
Reference: EJP72161

To appear in: *European Journal of Pharmacology*

Received date: 8 September 2018
Revised date: 8 January 2019
Accepted date: 15 January 2019

Cite this article as: Tao Li, Xiu-Ju Luo, E-Li Wang, Nian-Sheng Li, Xiao-Jie Zhang, Feng-Lin Song, Jin-Fu Yang, Bin Liu and Jun Peng, Magnesium lithospermate B prevents phenotypic transformation of pulmonary arteries in rats with hypoxic pulmonary hypertension through suppression of NADPH oxidase, *European Journal of Pharmacology,* https://doi.org/10.1016/j.ejphar.2019.01.020

Magnesium lithospermate B prevents phenotypic transformation of pulmonary arteries in rats with hypoxic pulmonary hypertension through suppression of NADPH oxidase

Tao Li[1], Xiu-Ju Luo[2], E-Li Wang[1], Nian-Sheng Li[1], Xiao-Jie Zhang[1], Feng-Lin Song[3], Jin-Fu Yang[3], Bin Liu[1,4*], Jun Peng[1,5*]

[1]Department of Pharmacology, Xiangya School of Pharmaceutical Sciences, Central South University, Changsha 410078, China.

[2]Department of Laboratory Medicine, the third Xiangya Hospital, Central South University, Changsha 410013，China.

[3]Department of cardiovascular surgery, the second Xiangya Hosptial, Central South University, 410011 Changsha China

[4]Department of Pharmacy, Xiangya Hospital, Central South University, Changsha 410008, China.

[5]Hunan Provincial Key Laboratory of Cardiovascular Research, School of Pharmaceutical Sciences, Central South University, Changsha 410078, China

liubin@csu.edu.cn

Junpeng@csu.edu.cn

[*]**Correspondence to**: Department of Pharmacy, Xiangya Hospital, Central South University, No. 87 Xiangya Road, Changsha, 410008, China.

[*]**Correspondence to**: Department of Pharmacology, School of Pharmaceutical Sciences, Central South University. No.110 Xiang-Ya Road, Changsha, 410078, China. Tel: 0086-731-82355080；Fax: 0086-731-82355078.

ABSTRACT

Magnesium lithospermate B (MLB) shows multiple biological activities including anti-oxidation and anti-proliferation in various diseases. However, the function of MLB in pulmonary arterial hypertension (PAH) is still unknown. This study aims to investigate the effect of MLB on hypoxia-induced phenotypic transformation of pulmonary arterial smooth muscle cells (PASMCs) and the underlying mechanisms. SD rats (or PASMCs) were exposed

to 10% O_2 for 3 weeks (or 3% O_2 for 48h) along with MLB or NADPH oxidase （NOX） inhibitor intervention. The effects of MLB on hemodynamics, pulmonary vascular remodeling and phenotypic transformation of PASMCs were observed first. Then, its effects on the protein levels of NOX (NOX2 and NOX4), ERK and p-ERK were examined. The results showed that MLB prevented the elevation in right ventricular systolic pressure and the increase in ratio of wall thickness to vessel external diameter of pulmonary arteries in PAH rats, and attenuated phenotypic transformation of PASMCs (decrease in α-smooth muscle actin while increase in osteopontin), accompanied by downregulation of NOX (NOX2 and NOX4) protein levels, decrease of ROS and H_2O_2 production, and suppression of the phosphorylation of ERK. NOX inhibitor (VAS2870) achieved similar results to that of MLB did in the hypoxia-treated PASMCs. Based on the observations, we conclude that MLB is able to prevent phenotypic transformation of pulmonary arteries in hypoxic PAH rats through suppression of NOX/ROS/ERK pathway, and MLB might have the potentials in PAH therapy.

Graphical abstract

fx1

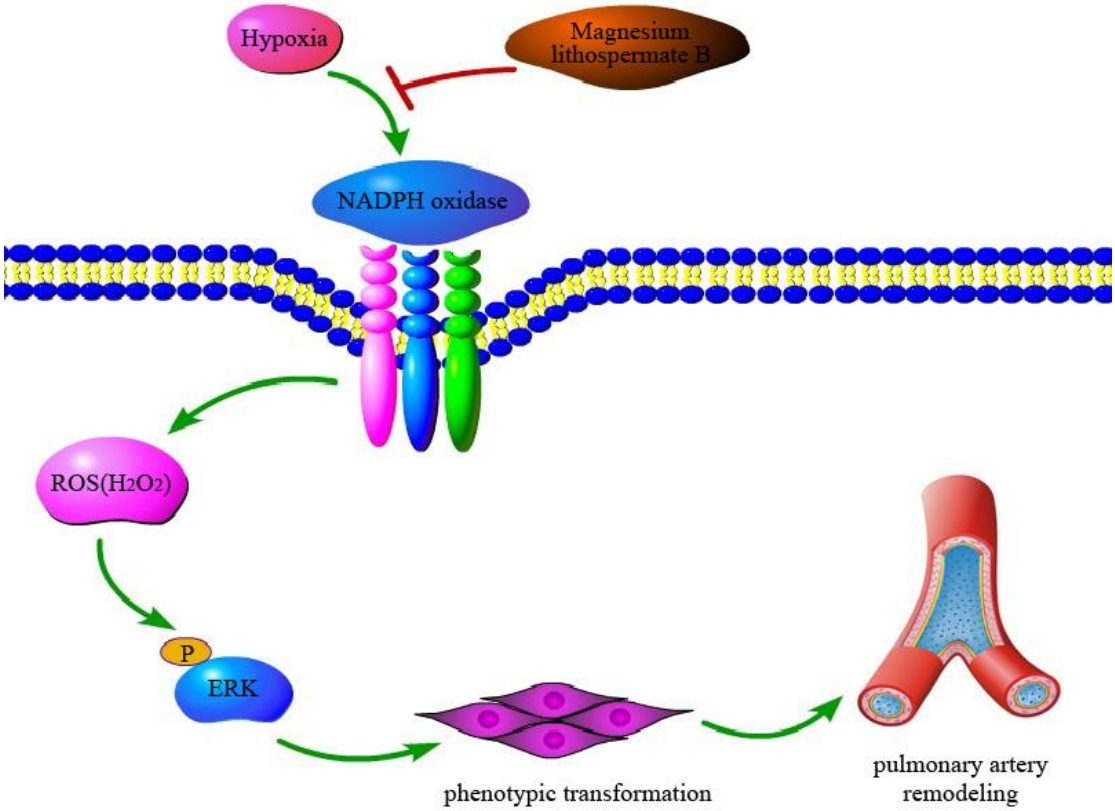

Key Words: Magnesium lithospermate B, pulmonary arterial hypertension, phenotypic transformation, pulmonary vascular remodeling, NADPH oxidase

1. Introduction

Pulmonary arterial hypertension (PAH) is a destructive and progressive disease characterized by elevation of pulmonary vascular resistance, which leads to increase of pulmonary arterial pressure and eventually right heart failure (Li et al., 2018). Pulmonary vascular remodeling is the major pathological features of PAH and the excessive proliferation of pulmonary artery smooth muscle cells (PASMCs) is an important factor contributing to vascular remodeling (Abe et al., 2010; Zurlo et al., 2018). PASMCs may undergo phenotypic transition from a differentiated phenotype (contractile phenotype) to a dedifferentiated phenotype (synthetic phenotype) in response to different stimuli such as hypoxia (Charles et

al., 2018; Xie et al., 2011). The contractile phenotype is characterized by high expression of contractile genes with a low rate of proliferation, such as α-smooth muscle actin (α-SMA) and smooth muscle 22α (SM22α). Conversely, synthetic phenotype expresses low level of contractile genes with a high rate of proliferation, such as osteopontin (OPN) and cyclin D1 (Owens et al., 2004). Therefore, the phenotypic transformation of PASMCs from contraction to synthesis is recognized as a key step for vascular remodeling in the development of PAH (Zhang et al., 2018b). However, the mechanisms responsible for phenotypic transformation of PASMCs are not fully understood.

There is evidence that reactive oxygen species (ROS) are involved in various aspects of pulmonary vasculature under physiological or pathological conditions, and NADPH oxidases (NOX) - derived products are considered as the primary source of ROS (Jin et al., 2016; Schroder et al., 2012). Reports from other labs and ours have repeatedly demonstrated that NOX are up-regulated in animals or humans with PAH, suggesting that NOX-derived ROS may contribute to the development of PAH (Jin et al., 2016; Liu et al., 2014; Schroder et al., 2012). For example, NOX-derived ROS can either cause endothelial dysfunction through oxidative injury or function as a signaling molecule to promote PASMCs proliferation and migration (Liu et al., 2016). Since phenotypic transformation from contraction to synthesis leads to acceleration of PASMCs proliferation, we thus hypothesize that NOX-derived ROS may contribute to phenotypic transformation of PASMCs in the development of PAH, and targeting NOX might be a useful strategy for PAH therapy.

Actually, NOX inhibitors, such as apocynin and diphenyleneiodonium, have been reported to be effective on PAH (Peng et al., 2017). However, most inhibitors used for NOX

intervention are not specific and they lack clinical value. Recently, we have found that magnesium lithospermate B (MLB), an active component of the water-soluble fraction of *Salvia miltiorrhiza*, might be a novel inhibitor of NOX because its protective effect on cerebral ischemia/reperfusion injury in rats was related to inhibition of NOX (Lou et al., 2015). In another report, MLB was able to prevent both injury-induced neointimal formation in vivo and platelet-derived growth factor (PDGF)-induced vascular smooth muscle cell proliferation in vitro (Hur et al., 2008). Based on these reports, we predict that MLB can prevent the development of PAH though mechanisms involving blocking the expression of NOX and the phenotypic transformation of PASMCs.

In the present study, by using a rat model of hypoxia-induced PAH, we investigated whether MLB was able to prevent the phenotypic transformation of pulmonary arteries and whether the preventive effect of MLB on PAH is related to suppression of NOX. By using an in vitro model of hypoxia-induced phenotypic transformation of PASMCs as well as the specific inhibitor of NOX (VAS2870), we verified the preventive effect of MLB on hypoxia-induced phenotypic transformation and the possible mechanisms.

2. Materials and methods

2.1. Ethics statement

Male Sprague-Dawley (SD) rats (180-220g) were obtained from Laboratory Animal Center, Xiangya School of Medicine, Central South University, China. All procedures performed on the rats were conducted according to the guidelines from the National Institutes of Health (NIH Publication, 8th edition, 2011) and the ARRIVE guidelines (Animal Research: Reporting In Vivo Experiments). The experiments were approved by the Central South

University Veterinary Medicine Animal Care and Use Committee.

2.2. Experimental protocol for animals

SD rats were randomly allocated to 4 groups as follows (n = 6 per group): a normoxia group, a hypoxia group, a hypoxia plus MLB (L) group, and a hypoxia plus MLB (H) group. For the normoxia group, rats were placed in a chamber with normobaric normoxia (21% O_2); for the hypoxia group, rats were placed in a chamber and exposed to 10% O_2 continuously for 3 weeks (the door of the chamber was opened for a while every day for supplementary feed and water as well as replacing cage bedding); for the hypoxia plus MLB (L) or MLB (H) group, rats were given MLB (purity≥90.0%, provided by Greenvalley Pharmaceutical Company, Shanghai, China) at dosage of 5 or 15 mg/kg/d (i.p., dissolved in normal saline) and subjected to hypoxia for 3 weeks. No animal was dead in all experimental groups in the whole process. At the end, the rats were anesthetized with pentobarbital (30 mg/kg, i.p.) and subjected to measurement of right ventricle systolic pressure (RVSP). After killing the anesthetized rats, the lungs were saved for hematoxylin-eosin, Masson staining and biochemical analysis (ROS level), and the pulmonary arterial tissues were isolated for molecular studies (relevant protein expression).

2.3. Experimental protocol for cultured cells

The in vitro experiments were designed to verify the effect of MLB on phenotypic transformation of PASMCs. The rat primary PASMCs were isolated from the pulmonary

arteries and the passage 3~6 cells were chosen for the following studies.

The first set of in vitro experiments was designed to optimize the condition for hypoxia-induced phenotypic transformation of PASMCs, which mimics the hypoxic treatment in vivo. The PASMCs were plated in 6-well plates and were quiescent for 24 h in DMEM supplemented with 0.1% serum. Then the cells were subjected to normoxia or hypoxia (3% O_2, 92% N_2 and 5% CO_2) treatment for 6h, 12h, 24h or 48h. At the end of experiments, cell viability and relevant protein levels for phenotypic transformation were measured. Based on the results from time-course experiments, the condition of 48h-hypoxia was chosen for the following cell culture studies. Under this time condition, a dose-effect relationship between MLB and PASMCs cell viability was performed. Based on this experiment, a concentration of 20 μM for MLB was chosen for the following cell culture experiments.

The second set of experiments was designed to evaluate the effect of MLB on hypoxia-induced phenotypic transformation of PASMCs and the potential mechanisms. The cells were divided into 5 groups (6 individual experiments per group): the control group, PASMCs were cultured under normal conditions; the hypoxia group, PASMCs were subjected to hypoxia for 48h; the hypoxia plus MLB group, MLB was added to the culture medium (20 μM, final concentration) before the hypoxia treatment; the hypoxia plus VAS2870 (a specific inhibitor of NOX, dissolved in DMSO) group, VAS2870 was added to the culture medium (10 μM, final concentration) before the hypoxia treatment; and the hypoxia plus vehicle group, equal volume of vehicle (DMSO) was added to culture medium before the hypoxia treatment. At the end of experiments, the cells were collected for

biochemical analysis (ROS level and H_2O_2 concentration) and molecular studies (relevant protein expression).

2.4. Hematoxylin-eosin (HE) and Masson' trichrome staining

To compare the morphological changes in pulmonary arteries among the experimental groups, HE staining was performed. Briefly, lung tissues were fixed with 4% paraformaldehyde and embedded in paraffin and then cut into 5μm sections. The slices were stained with HE (Beyotime, Jiangsu, China) and a minimum of 10 microscopic fields from each slide were randomly selected for observation under a microscope (Olympus Corporation, Tokyo, Japan). For quantitation of pulmonary arterial wall thickness, the lumen diameter (or area at the level of the basement membrane) and total vascular diameter (or area at the adventitial border) in 10 muscular arteries with diameter of 50-100 μm per lung section were outlined. The diameters and area sizes were measured with Image J (NIH, USA). The vascular wall thickness was calculated as follows: wall thickness (WT) = (total vascular diameter – lumen diameter)/ total vascular diameter; wall area (WA) = (total vascular area – lumen area)/ total vascular area.

To determine the extent of collagen deposition in pulmonary arterioles, Masson' trichrome staining was performed following the instruction provided by the kit supplier (Baso Biotech, Zhuhai, China).

2.5. Cell viability assay

Cell viability was measured with a MTS Assay Kit according to the protocol provided by the manufacturer (Promega, USA). Briefly, PASMCs were seeded at the 96-well plates and

starved for 24 h. Then MTS was added to culture medium DMEM [MTS: DMEM (v/v) = 1:10 per well]. The cells were incubated at 37°C for 2.5 h and the absorbance was examined at 490nm by a spectrophotometer.

2.6. Cell proliferation assay

The proliferation of PASMCs was evaluated with EdU Incorporation Assay Kit following the protocol provided by the manufacturer (RiboBio Co. Ltd., Guangzhou, China). In brief, EdU (50 μM) was added to the culture medium and incubated at 37°C for 2 h. Then the cells were fixed, stained, and imaged by fluorescent microscopy (Olympus IX71, Japan). The EdU-positive cells were counted and normalized to the total number of DAPI-stained cells.

2.7. Detection of reactive oxygen species (ROS) level

The ROS level in lung tissues was detected by using dihydroethidium staining assay. In brief, lung tissues were cut into 5μm-thick sections. The slices were stained with dihydroethidium (10 μM) (Beyotime, Jiangsu, China) and then were incubated at 37 °C for 30 min in a dark humidified chamber. The fluorescence of ethidium were randomly selected for observation under a microscope (Olympus IX71, Japan).

The measurement of intracellular ROS levels was dependent on the fluorescent signal of 2',7'-dichlorodihydrofluorescein diacetate (DCFH-DA), a cell-permeable indicator of ROS (Beyotime, Jiangsu, China). DCFH-DA is nonfluorescent until the acetate groups are removed by intracellular ROS. Briefly, PASMCs were washed with PBS and incubated with

DCFH-DA (10 μM) at 37℃ for 20 min. Then, the ROS-mediated fluorescence was observed under a fluorescent microscope with excitation set at 502 nm and emission set at 523 nm.

2.8. Measurement of hydrogen peroxide (H_2O_2) content

The detection of H_2O_2 is based on oxidation of ferrous (Fe^{2+}) to ferric ion (Fe^{3+}) in the presence of xylenol orange. In a sulfuric acid solution, the Fe^{3+} complexes with the xylenol orange dye to yield a purple product with maximum absorbance at 560 nm. For measurement of H_2O_2 level, 50 μL of supernatant of pulmonary tissue or PASMCs homogenates and 100 μL of work solution (0.25mM ammonium ferrous II sulfate, 25mM H_2SO_4, 100 mM sorbitol, 125 μM xylenol orange) were mixed and incubated at room temperature for 20 min. The change of absorbance at 560 nm was monitored and the levels of H_2O_2 were calculated according to a standard curve made from the standard solutions provided by the supplier (Beyotime, Jiangsu, China).

2.9. Western blot analysis

Pulmonary arterial tissues or PASMCs were homogenized in ice-cold lysis buffer (250 mmol/L Tris-HCl, pH 6.8; 4% SDS, 20% vol/vol glycerol and Roche EDTA-free protease inhibitor cocktail) and sonicated for ~1 min, then centrifuged for 15 min at 15000g. The protein concentration in homogenate was determined by a BCA Protein Assay kit (Beyotime, Jiangsu, China). Western blot were performed according to standard techniques. Briefly, samples containing 20 - 60 μg of protein were subjected to SDS-PAGE (10% gel) and they were transferred to polyvinylidene fluoride (PVDF) membranes. The blots were then

incubated with primary antibodies against NOX2 (Santa Cruz, CA, USA), NOX4 (Santa Cruz, CA, USA), SM22α (Abcam, Cambridge, MA, USA), α-SMA (BOSTER, Wuhan, China), OPN (Abcam, Cambridge, MA, USA), cyclin D1 (BOSTER, Wuhan, China) or ERK/p-ERK (Cell Signaling Technology, Danvers, USA) followed by HRP-conjugated secondary antibodies (Beyotime, Jiangsu, China). The signals were detected by Luminata™ Creseendo Western HRP substrate through Molecular Imager ChemiDoc XRS System (Bio-Rad, Philadelphia, PA). The densitometric quantification was conducted with Image J (NIH, USA). Antibodies against β-actin (Beyotime, Jiangsu, China) were used as loading controls.

2.10. Statistical analysis

SPSS software (Version 20) was used for statistical analysis. Data were expressed as mean ± S.E.M.. Differences in values among the multiple groups were determined by the analysis of variance with Bonferroni's multiple comparison tests. Differences were considered significant when $P < 0.05$.

3. Results

3. 1. MLB prevented the development of hypoxia-induced pulmonary hypertension

Pulmonary hypertension was developed after the rats continuously exposed to hypoxia (10% O_2) for 3 weeks. Compared with the normoxia group, the right ventricular systolic pressure (RVSP) in the hypoxia group were significantly elevated; these phenomena were markedly attenuated by MLB in a dose-dependent manner (5 and 15 mg/kg) (Fig. 1 A and B).

As shown in Fig. 1 C-E, the ratio of wall thickness to vessel external diameter (WT %)

and the ratio of wall area to total vessel area (WA %) in the small pulmonary arteries were significantly increased in the hypoxia-treated rats as compared with that in the normoxia group. The hypoxia-induced pulmonary vascular remodeling was reduced by MLB in a dose-dependent manner. Consistent with the vascular remodeling, Masson' trichrome staining showed that the increased collagen deposition around pulmonary vessels in hypoxia-treated rats, these phenomena were attenuated in the presence of MLB (Fig. 1 F).

3.2. MLB suppressed hypoxia-induced phenotypic transformation of pulmonary arteries

As shown in Fig.2, pulmonary arteries from hypoxia-treated rats exhibited phenotypic transformation from a contractile to a synthetic type, as evidenced by down-regulation of contractile proteins α-smooth muscle actin (α-SMA) and smooth muscle 22α (SM22α) while up-regulation of the synthetic protein osteopontin (OPN) and proliferative protein cyclin D1. The hypoxia-induced phenotypic transformation of pulmonary arteries was suppressed by MLB in a dose-dependent manner.

3.3. MLB blocked hypoxia-induced NOX expression and ERK phosphorylation in pulmonary arteries

Compared to the normoxia group, hypoxia treatment caused a significant increase in NOX (NOX2 and NOX4) protein levels in the pulmonary arteries of rats, which was blocked by MLB in a dose-dependent manner (Fig.3 A and B). Consistently, ROS level and H_2O_2 content (a NOX - derived product) in the hypoxia group was significantly increased (Fig.3 C and D); this phenomenon was reversed in the presence of MLB. Moreover, the

phosphorylation level of ERK (p-ERK) in pulmonary arteries was apparently elevated in hypoxia-treated rats, which was blocked in the presence of MLB (Fig.3 E). However, there was no change in total ERK level in all groups.

3.4. Establishment of hypoxia-induced phenotypic transformation of PASMCs in vitro

Primary PASMCs were cultured under hypoxic condition for 6h, 12h, 24h or 48h to establish an in vitro model of phenotypic transformation. As shown in Fig. 4, compared to the normoxia group, the cell viability was increased in a time course-dependent manner concomitant with a down-regulation of the contractile proteins α-SMA and SM22α while up-regulation of the synthetic protein OPN and proliferative protein cyclin D1, suggesting the establishment of hypoxia-induced phenotypic transformation of PASMCs in vitro was successful. Based on the results, the 48h-hypoxia was chosen for the following cell culture studies. Under this time condition, MLB suppressed hypoxia-induced PASMCs proliferation in a dose-dependent manner with IC_{50} at ~ 60.75 μM (Figure S1). Based on this experiment, we chose MLB at 20 μM for the following cell culture experiments.

3.5. MLB inhibited hypoxia-induced phenotypic transformation of PASMCs in vitro

Consistent with the results in vivo, the hypoxia-treated PASMCs exhibited phenotypic transformation from a contractile to a synthetic type, as evidenced by down-regulation of the contractile proteins α-SMA and SM22α while up-regulation of the synthetic protein OPN. The hypoxia-induced phenotypic transformation of PASMCs was inhibited in the presence of MLB. Similarly, VAS2870, a specific inhibitor of NOX, could also suppress the

hypoxia-induced phenotypic transformation, but the vehicle of VAS2870 has no such effect (Fig. 5 A-C).

In agreement with results of hypoxia-induced phenotypic transformation, PASMCs proliferation was significantly accelerated under hypoxic condition, as revealed by an increase in the EdU-positive cells and the proliferative protein cyclin D1; these phenomena were attenuated in the presence of MLB or VAS2870, but the vehicle of VAS2870 did not show such effect (Fig. 5 D-F).

3.6. MLB suppressed hypoxia-induced NOX expression and ERK phosphorylation in PASMCs in vitro

Consistent with the results in vivo, the hypoxia-treated PASMCs exhibited up-regulation of NOX2 and NOX4 (Fig.6 A and B), accompanied by an increase in ROS level in cells and H_2O_2 contents in both culture medium and cells (Fig. 6 C-E); these increases were suppressed in the presence of MLB or VAS2870. Furthermore, the levels of p-ERK in hypoxia-treated PASMCs was apparently elevated, which was attenuated in the presence of MLB or VAS2870 (Fig. 6 F). However, there was no change in total ERK level in all groups.

4. Discussion

In this study, we explored the effects of MLB on hypoxia-induced phenotypic transformation of PASMCs and the underlying mechanisms. Our data showed that administration of MLB significantly prevented phenotypic transformation of pulmonary arteries in PAH rats, accompanied by a decrease in pulmonary vascular remodeling while an

increase in NOX (NOX2 and NOX4) protein expression and H_2O_2 production; these in vivo findings were further confirmed in hypoxia-treated PASMCs in vitro. To the best of our knowledge, this is the first study to provide evidence that MLB may exert preventive effect on PAH through prevention of phenotypic transformation of PASMCs; this effect is related to down-regulation of NOX2 and NOX4.

Pulmonary artery remodeling is a basic pathological characteristic for PAH (Ranchoux et al., 2015). In this study, rats continuously exposed to hypoxia for 3 weeks significantly induced pulmonary artery remodeling, evidenced by an increase in the ratio of wall thickness to vessel external diameter and the ratio of wall area to total vessel area in the small pulmonary arteries, concomitant with an elevation in the right ventricular systolic pressure, indicating the PAH animal model was successfully established.

It is well recognized that hypoxia-induced hyperproliferation of PASMCs is a major initial factor for pulmonary vascular remodeling in PAH (Zhang et al., 2018a). Different from cardiac cells and skeletal muscle cells, smooth muscle cells can undergo phenotypic changes under pathological conditions. For example, under hypoxic condition, PASMCs accelerate the phenotypic transformation from contractile to synthetic phenotype. This phenotypic switching obviously alters the functions of PASMC because the synthetic PASMCs migrate and proliferate more easily than contractile ones. Moreover, synthetic PASMCs can produce up to 25 to 46-fold more collagen than contractile ones, all of which contribute to pulmonary vascular remodeling in PAH (Owens et al., 2004). Consistent with the reports, the results of the present study demonstrated a down-regulation of contractile proteins and an up-regulation of synthetic proteins in the pulmonary arteries from hypoxia-treated rats, accompanied by a

phenotype of vascular remodeling. Based on these results, it naturally thinks that prevention of phenotypic transformation of PASMCs by a drug may have a promising prospect for PAH therapy. In the present study, our results indeed showed that MLB significantly prevented phenotypic transformation of pulmonary arteries from contractile to synthetic phenotype in PAH rats concomitant with improved pathological characteristics (decrease in RVSP, WT % and WA %), supporting that MLB might be a potential candidate for the prevention and treatment of PAH. However, the underlying mechanisms remain to be determined. It is noteworthy that we only showed the preventive effect of MLB on PAH in the present study. Although it might be able to exert therapeutic effect on PAH, further studies are necessary before drawing a firm conclusion.

MLB is a water-soluble active ingredient from Danshen. Early studies mainly focused on the lipophilic compounds of Danshen while recent studies have turned to hydrophilic compounds. So far, at least 50 chemical constituents have been isolated and identified from the aqueous extracts of Danshen. Among them, MLB is a major hydrophilic compound of Danshen and preserves its most pharmacological activities, such as anti-vasospasm, anti-inflammation and anti-oxidation (Chang et al., 2011; Lou et al., 2015; Park et al., 2017). There was evidence that MLB could inhibit PDGF-induced vascular smooth muscle cell proliferation and migration by suppressing ROS production (Hur et al., 2008). Based on this report, we hypothesize that MLB prevent phenotypic transformation of pulmonary arteries in PAH rats through a mechanism involving its anti-oxidative property. As a major source of ROS in cardiovascular system, NOX (particularly the NOX2 and NOX4 subunits) are activated under multiple pathological conditions (Liu et al., 2014; Ma et al., 2013).

NOX-derived ROS contribute to pulmonary artery remodeling, endothelial dysfunction, myocardial or cerebral ischemia/reperfusion injury (Lou et al., 2015; Zhang et al., 2012). We thus examined the correlation between MLB and NOX. We have found that MLB could significantly block NOX2 and NOX4 expression in pulmonary arteries of PAH rats concomitant with a decrease in H_2O_2 content, which confirmed our hypothesis before.

It is well known that ROS not only cause oxidative injury but also function as a second messenger to regulate intracellular signaling pathways (Vara and Pula, 2014). Thus, we focused on identification of the potential signaling molecules that involves in phenotypic transformation of pulmonary arteries in PAH rats. As a member of MAPK, ERK plays a key role in regulation of proliferation and migration in different type of cells (Sun et al., 2015). Since H_2O_2 is able to activate ERK in human pulmonary artery smooth muscle cell under hypoxic condition (Bijli et al., 2015), we therefore examined the effect of MLB on ERK phosphorylation in rat pulmonary artery. The results from the present study really showed that the levels of p-ERK in pulmonary arteries were apparently elevated in the hypoxia-treated rats, which were reversed in the presence of MLB. These results indicate that MLB prevents phenotypic transformation of pulmonary arteries in PAH rats through suppressing the NOX/ROS/ERK pathway. Previous report showed that MLB was able to decrease endothelin-1 through an NO-dependent mechanism, which led to reduction of experimental vasospasm in rats (Chang et al., 2011). Since endothelin-1 plays an important role in PAH development, thereby we could not rule out the possibility that the inhibitory effect of MLB on phenotypic transformation of pulmonary arteries in PAH rats might be also related to decrease of endothelin-1 production.

To further confirm our findings in vivo, we performed cell experiments in primary cultured PASMCs with MLB and VAS2870 (a NOX specific inhibitor). Here, VAS2870 was used as the a positive control for NOX inhibition (Lou et al., 2015). Consistent with the findings in vivo, the primary cultured PASMCs displayed phenotypic transformation from a contractile to a synthetic type concomitant with an up-regulation of NOX(NOX2 and NOX4) and an increase in H_2O_2 production as well as an elevation in p-ERK level; these phenomena were attenuated in the presence of MLB or VAS2870.

In conclusion, the results from this study have demonstrated for the first time that MLB exerts the preventive effect on PAH through blocking the phenotypic transformation of pulmonary arteries; and this action is related to suppression of the NOX/ROS/ERK pathway. Therefore, MLB may have the potential value in clinic for PAH prevention and/or therapy.

Acknowledgements

This work was supported by National Natural Science Foundation of China (No. 81703516 to Bin Liu, No. 81573430 to Xiu-Ju Luo, No. 81872873 to Jun Peng), Major Research Plan of the National Natural Science Foundation of China (No. 91439104 to Jun Peng; No. 91539111 to Jin-Fu Yang).

Author Agreement

We state here that all authors have seen and approved the final version of the manuscript being submitted. They warrant that the article is the authors' original work, hasn't received prior publication and isn't under consideration for publication elsewhere.

References

Abe, K., Toba, M., Alzoubi, A., Ito, M., Fagan, K.A., Cool, C.D., Voelkel, N.F., McMurtry, I.F., Oka, M., 2010. Formation of plexiform lesions in experimental severe pulmonary arterial hypertension. Circulation 121, 2747-2754.

Bijli, K.M., Kleinhenz, J.M., Murphy, T.C., Kang, B.Y., Adesina, S.E., Sutliff, R.L., Hart, C.M., 2015. Peroxisome proliferator-activated receptor gamma depletion stimulates Nox4 expression and human pulmonary artery smooth muscle cell proliferation. Free Radic Biol Med 80, 111-120.

Chang, C.Z., Wu, S.C., Kwan, A.L., Hwang, S.L., Howng, S.L., 2011. Magnesium lithospermate B alleviates the production of endothelin-1 through an NO-dependent mechanism and reduces experimental vasospasm in rats. Acta neurochirurgica 153, 2211-2217.

Charles, R., Bourmoum, M., Claing, A., 2018. ARF GTPases control phenotypic switching of vascular smooth muscle cells through the regulation of actin function and actin dependent gene expression. Cell Signal 46, 64-75.

Hur, K.Y., Seo, H.J., Kang, E.S., Kim, S.H., Song, S., Kim, E.H., Lim, S., Choi, C., Heo, J.H., Hwang, K.C., Ahn, C.W., Cha, B.S., Jung, M., Lee, H.C., 2008. Therapeutic effect of magnesium lithospermate B on neointimal formation after balloon-induced vascular injury. Eur J Pharmacol 586, 226-233.

Jin, H., Liu, M., Zhang, X., Pan, J., Han, J., Wang, Y., Lei, H., Ding, Y., Yuan, Y., 2016. Grape seed procyanidin extract attenuates hypoxic pulmonary hypertension by inhibiting oxidative stress and pulmonary arterial smooth muscle cells proliferation. J Nutr

Biochem 36, 81-88.

Li, Y., Li, L., Qian, Z., Lin, B., Chen, J., Luo, Y., Qu, J., Raj, J.U., Gou, D., 2018. Phosphatidylinositol 3-Kinase-DNA Methyltransferase 1-miR-1281-Histone Deacetylase 4 Regulatory Axis Mediates Platelet-Derived Growth Factor-Induced Proliferation and Migration of Pulmonary Artery Smooth Muscle Cells. J Am Heart Assoc 7.

Liu, B., Li, T., Peng, J.J., Zhang, J.J., Liu, W.Q., Luo, X.J., Ma, Q.L., Gong, Z.C., Peng, J., 2016. Non-muscle myosin light chain promotes endothelial progenitor cells senescence and dysfunction in pulmonary hypertensive rats through up-regulation of NADPH oxidase. Eur J Pharmacol 775, 67-77.

Liu, B., Luo, X.J., Yang, Z.B., Zhang, J.J., Li, T.B., Zhang, X.J., Ma, Q.L., Zhang, G.G., Hu, C.P., Peng, J., 2014. Inhibition of NOX/VPO1 pathway and inflammatory reaction by trimethoxystilbene in prevention of cardiovascular remodeling in hypoxia-induced pulmonary hypertensive rats. J Cardiovasc Pharmacol 63, 567-576.

Lou, Z., Ren, K.D., Tan, B., Peng, J.J., Ren, X., Yang, Z.B., Liu, B., Yang, J., Ma, Q.L., Luo, X.J., Peng, J., 2015. Salviaolate Protects Rat Brain from Ischemia-Reperfusion Injury through Inhibition of NADPH Oxidase. Planta Med 81, 1361-1369.

Ma, Q.L., Zhang, G.G., Peng, J., 2013. Vascular peroxidase 1: a novel enzyme in promoting oxidative stress in cardiovascular system. Trends Cardiovasc Med 23, 179-183.

Owens, G.K., Kumar, M.S., Wamhoff, B.R., 2004. Molecular regulation of vascular smooth muscle cell differentiation in development and disease. Physiological reviews 84, 767-801.

Park, C.H., Shin, S.H., Lee, E.K., Kim, D.H., Kim, M.J., Roh, S.S., Yokozawa, T., Chung,

H.Y., 2017. Magnesium Lithospermate B from Salvia miltiorrhiza Bunge Ameliorates Aging-Induced Renal Inflammation and Senescence via NADPH Oxidase-Mediated Reactive Oxygen Generation. Phytother Res 31, 721-728.

Peng, J.J., Liu, B., Xu, J.Y., Peng, J., Luo, X.J., 2017. NADPH oxidase: its potential role in promotion of pulmonary arterial hypertension. Naunyn Schmiedebergs Arch Pharmacol 390, 331-338.

Ranchoux, B., Antigny, F., Rucker-Martin, C., Hautefort, A., Pechoux, C., Bogaard, H.J., Dorfmuller, P., Remy, S., Lecerf, F., Plante, S., Chat, S., Fadel, E., Houssaini, A., Anegon, I., Adnot, S., Simonneau, G., Humbert, M., Cohen-Kaminsky, S., Perros, F., 2015. Endothelial-to-mesenchymal transition in pulmonary hypertension. Circulation 131, 1006-1018.

Schroder, K., Zhang, M., Benkhoff, S., Mieth, A., Pliquett, R., Kosowski, J., Kruse, C., Luedike, P., Michaelis, U.R., Weissmann, N., Dimmeler, S., Shah, A.M., Brandes, R.P., 2012. Nox4 is a protective reactive oxygen species generating vascular NADPH oxidase. Circ Res 110, 1217-1225.

Sun, Y., Liu, W.Z., Liu, T., Feng, X., Yang, N., Zhou, H.F., 2015. Signaling pathway of MAPK/ERK in cell proliferation, differentiation, migration, senescence and apoptosis. J Recept Signal Transduct Res 35, 600-604.

Vara, D., Pula, G., 2014. Reactive oxygen species: physiological roles in the regulation of vascular cells. Curr Mol Med 14, 1103-1125.

Xie, C., Ritchie, R.P., Huang, H., Zhang, J., Chen, Y.E., 2011. Smooth muscle cell differentiation in vitro: models and underlying molecular mechanisms. Arterioscler

Thromb Vasc Biol 31, 1485-1494.

Zhang, N., Dong, M., Luo, Y., Zhao, F., Li, Y., 2018a. Danshensu prevents hypoxic pulmonary hypertension in rats by inhibiting the proliferation of pulmonary artery smooth muscle cells via TGF-beta-smad3-associated pathway. Eur J Pharmacol 820, 1-7.

Zhang, W., Zhu, T., Wu, W., Ge, X., Xiong, X., Zhang, Z., Hu, C., 2018b. LOX-1 mediated phenotypic switching of pulmonary arterial smooth muscle cells contributes to hypoxic pulmonary hypertension. Eur J Pharmacol 818, 84-95.

Zhang, Y.S., He, L., Liu, B., Li, N.S., Luo, X.J., Hu, C.P., Ma, Q.L., Zhang, G.G., Li, Y.J., Peng, J., 2012. A novel pathway of NADPH oxidase/vascular peroxidase 1 in mediating oxidative injury following ischemia-reperfusion. Basic Res Cardiol 107, 266.

Zurlo, G., Piquereau, J., Moulin, M., Pires Da Silva, J., Gressette, M., Ranchoux, B., Garnier, A., Ventura-Clapier, R., Fadel, E., Humbert, M., Lemaire, C., Perros, F., Veksler, V., 2018. Sirtuin 1 regulates pulmonary artery smooth muscle cell proliferation: role in pulmonary arterial hypertension. J Hypertens 36, 1164-1177.

Figure 1. MLB prevented the development of hypoxia-induced pulmonary hypertension

A. Representative images for the recording of RVSP. B. The value of RVSP. C. Representative images of HE staining for lung tissues (arrows indicate the pulmonary artery). D. The ratio of wall thickness to total vessel external diameter for pulmonary artery. E. The ratio of wall area to total vessel area for pulmonary artery. F. Representative images of Masson' trichrome staining for lung tissues. The data are presented as mean ± S.E.M.(n=6 per group). MLB, Magnesium lithospermate B; RVSP, right ventricle systolic pressure; +MLB(L):

hypoxia + MLB (5mg/kg/d); +MLB(H): hypoxia + MLB (15mg/kg/d). $^{**}P < 0.01$ *vs* Normoxia; $^{\#\#}P < 0.01$ *vs* Hypoxia.

Figure 2. MLB suppressed hypoxia-induced phenotypic transformation of pulmonary arteries The protein levels of α-SMA (A), SM22α (B), osteopontin (OPN, C) and cyclin D1 (D). Top, optical density of protein band. Bottom, representative images of Western blot. All values are expressed as mean ± S.E.M. (n=6 per group). MLB, Magnesium lithospermate B; +MLB(L): hypoxia + MLB (5mg/kg/d); +MLB(H): hypoxia + MLB (15mg/kg/d). $^{**}P < 0.01$ *vs* Normoxia; $^{\#}P < 0.05$ *vs* Hypoxia.

Figure 3. MLB blocked hypoxia-induced NOX expression and ERK phosphorylation in pulmonary arteries. The protein levels of NOX2 (A) and NOX4 (B) in pulmonary arteries. Top, optical density of protein band. Bottom, representative images of Western blot. C. Detection of ROS level in lung tissues by dihydroethidium staining. D. H_2O_2 content in lung tissues. E. The protein levels of p-ERK and ERK in pulmonary arteries. Top, optical density of protein band. Bottom, representative images of Western blot. All values are expressed as mean ± S.E.M.(n=6 per group). MLB, Magnesium lithospermate B; +MLB(L): hypoxia + MLB (5mg/kg/d); +MLB(H): hypoxia + MLB (15mg/kg/d). $^{**}P < 0.01$*vs* Normoxia; $^{\#}P < 0.05$, $^{\#\#}P < 0.01$*vs* Hypoxia.

Figure 4. Establishment of hypoxia-induced phenotypic transformation of PASMCs in vitro A. Cell viability under hypoxic condition at different time points (n=5 per group). B-E.

the protein levels of α-SMA, SM22α, osteopontin (OPN) and cyclin D1 in PASMCs under hypoxic condition at different time points (n=3 per group). Top, optical density of protein band. Bottom, representative images of Western blot. Data are presented as means ± S.E.M.. $^{*}P<0.05$, $^{**}P < 0.01$*vs* Normoxia.

Figure 5. MLB inhibited phenotypic transformation and proliferation in hypoxia-treated PASMCs in vitro The protein levels of α-SMA (A), SM22α (B) and osteopontin (OPN, C) in PASMCs. Top, optical density of protein band. Bottom, representative images of Western blot. D. Representative images of EdU assay for PASMCs. E. Percentage of EdU-positive cells. F. Cyclin D1 protein level in PASMCs. Top, optical density of protein band. Bottom, representative images of Western blot. All values are expressed as mean ± S.E.M.(n=3 per group). MLB, Magnesium lithospermate B; +MLB: hypoxia + MLB; +VAS2870: hypoxia+VAS2870; +Vehicle: hypoxia +vehicle of VAS2870 (DMSO). $^{**}P < 0.01$ *vs* Normoxia; $^{\#}P<0.05$ *vs* Hypoxia.

Figure 6. MLB suppressed NOX expression and ERK phosphorylation in hypoxia-treated PASMCs in vitro. The protein levels of NOX2 (A) and NOX4 (B). Top, optical density of protein band. Bottom, representative images of Western blot. C. Representative images for ROS detection with DCFH-DA in PASMCs. D. H_2O_2 level in culture medium. E. H_2O_2 content in PASMCs. F. The protein levels of p-ERK and ERK in PASMCs. Data are expressed as mean ± S.E.M. (n=3 per group). MLB, Magnesium lithospermate B; +MLB: hypoxia + MLB; +VAS2870: hypoxia+VAS2870; +vehicle: hypoxia +vehicle of VAS2870 (DMSO). $^{**}P < 0.01$ *vs* Normoxia; $^{\#}P<0.05$ *vs* Hypoxia.

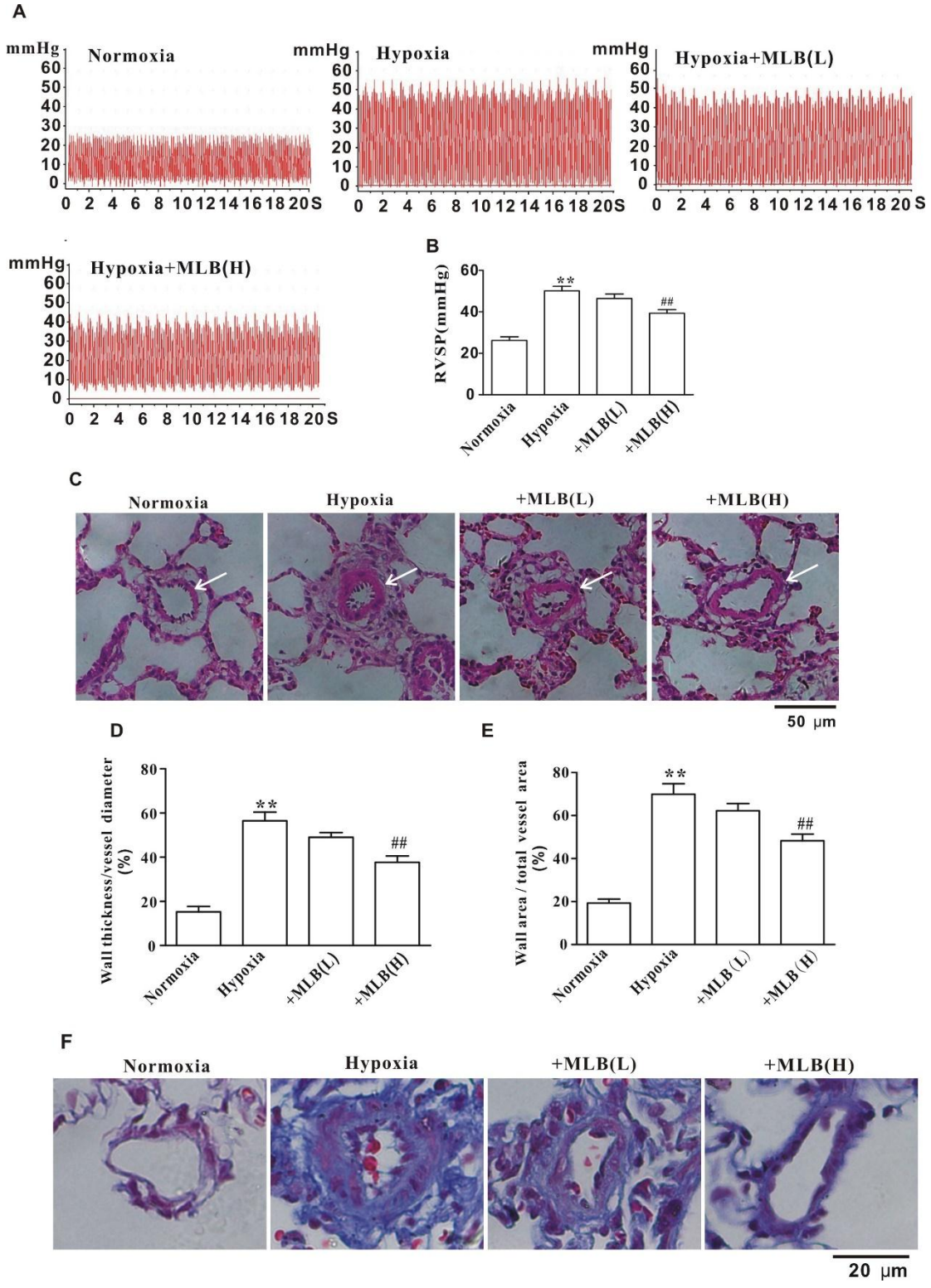

Figure 1

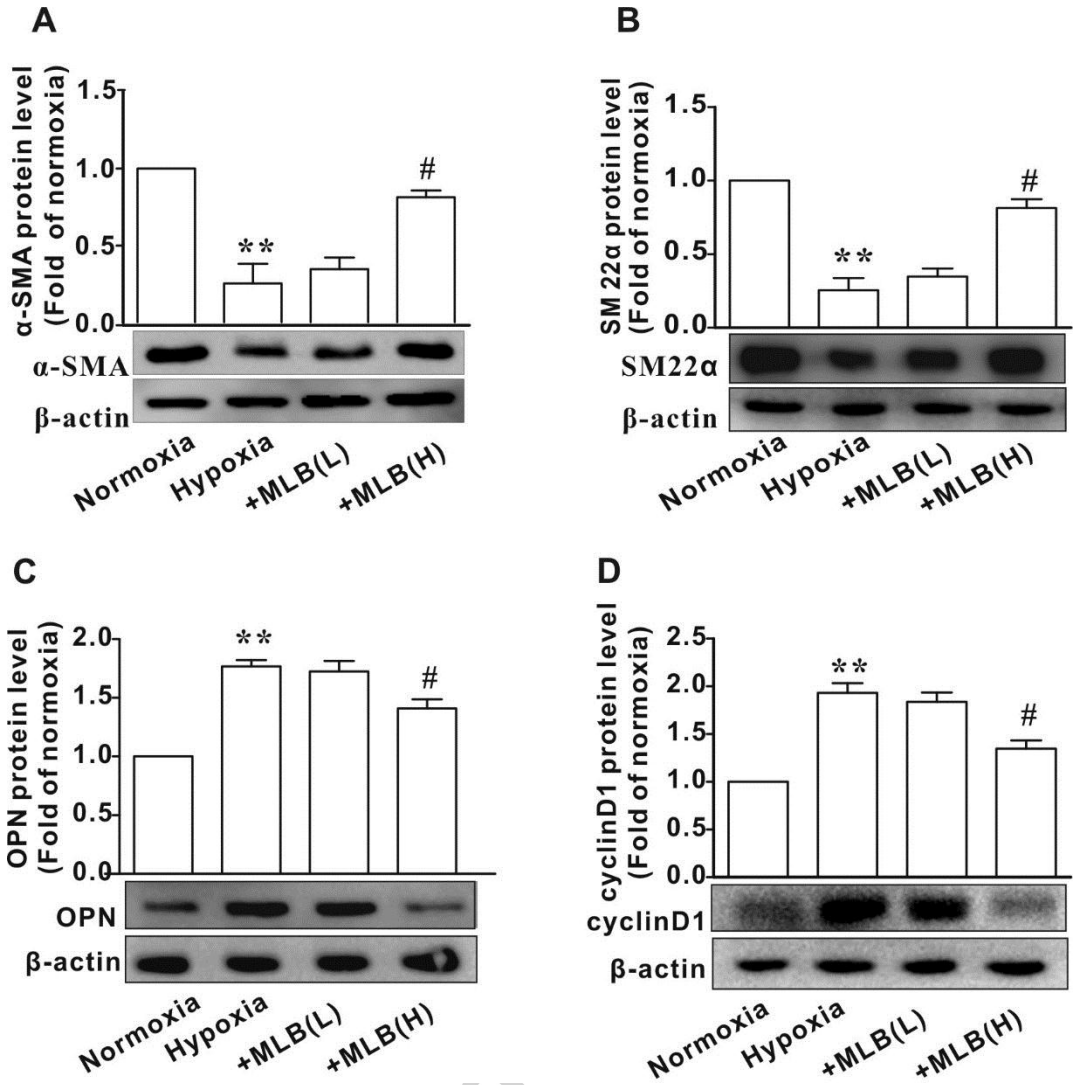

Figure 2

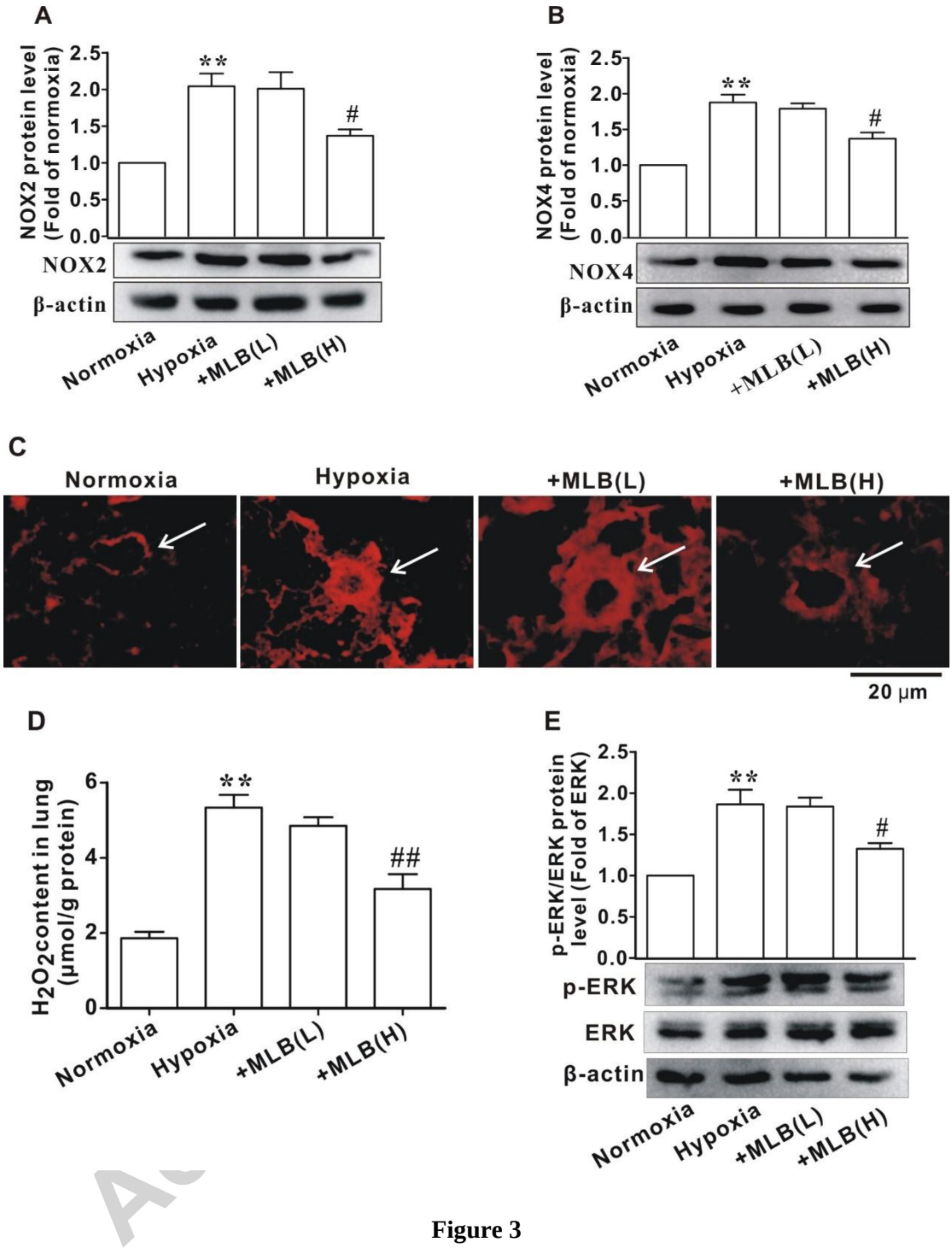

Figure 3

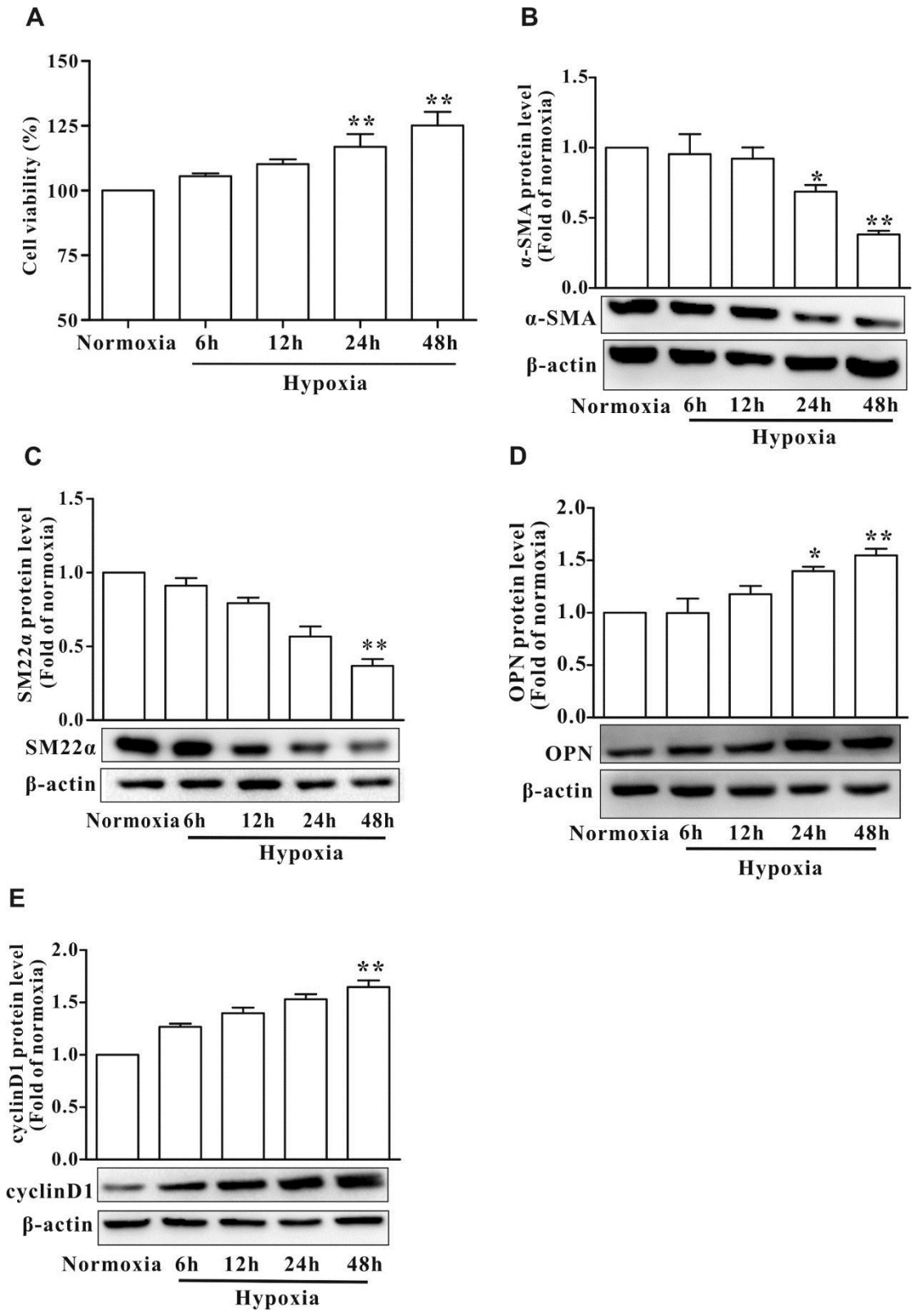

Figure 4

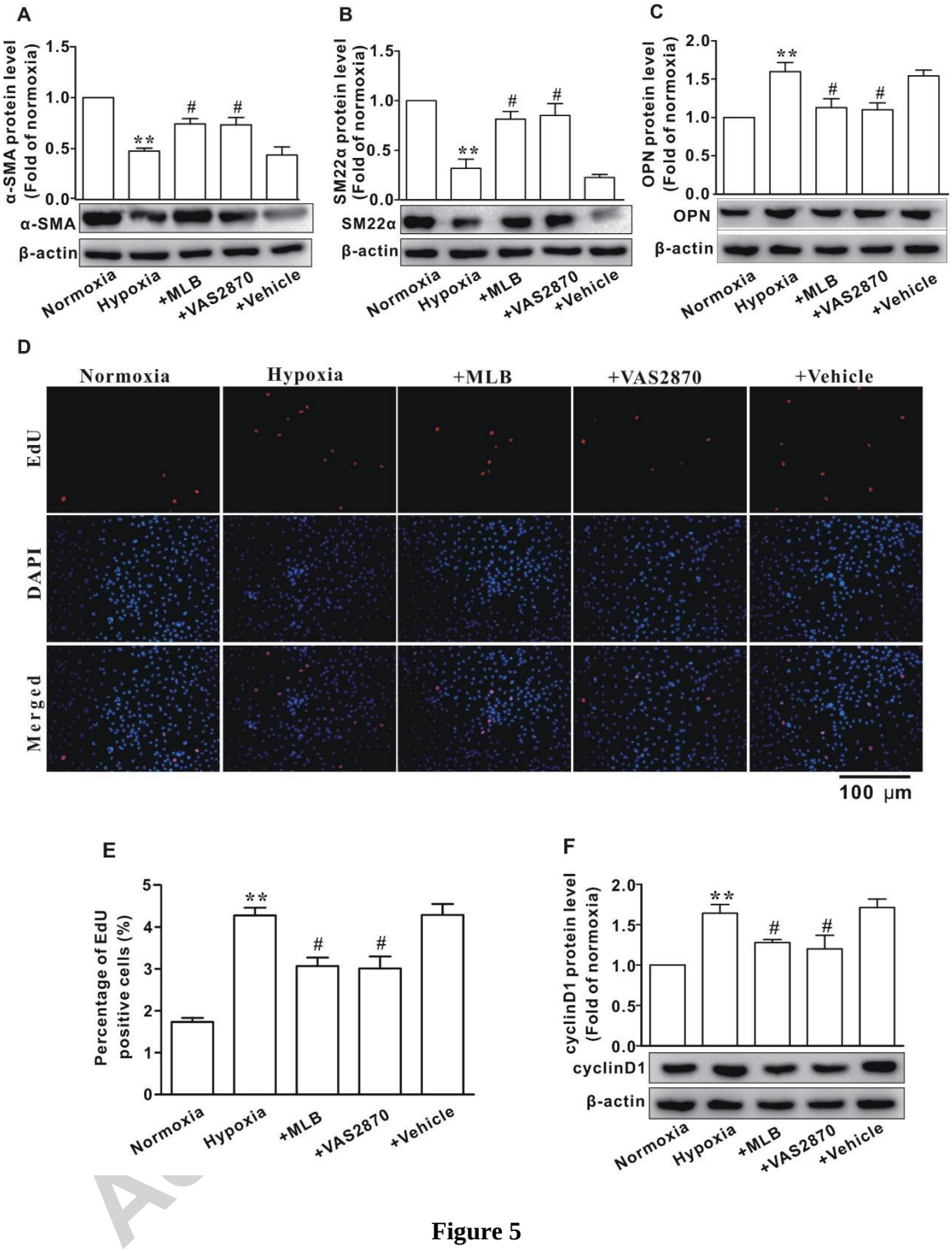

Figure 5

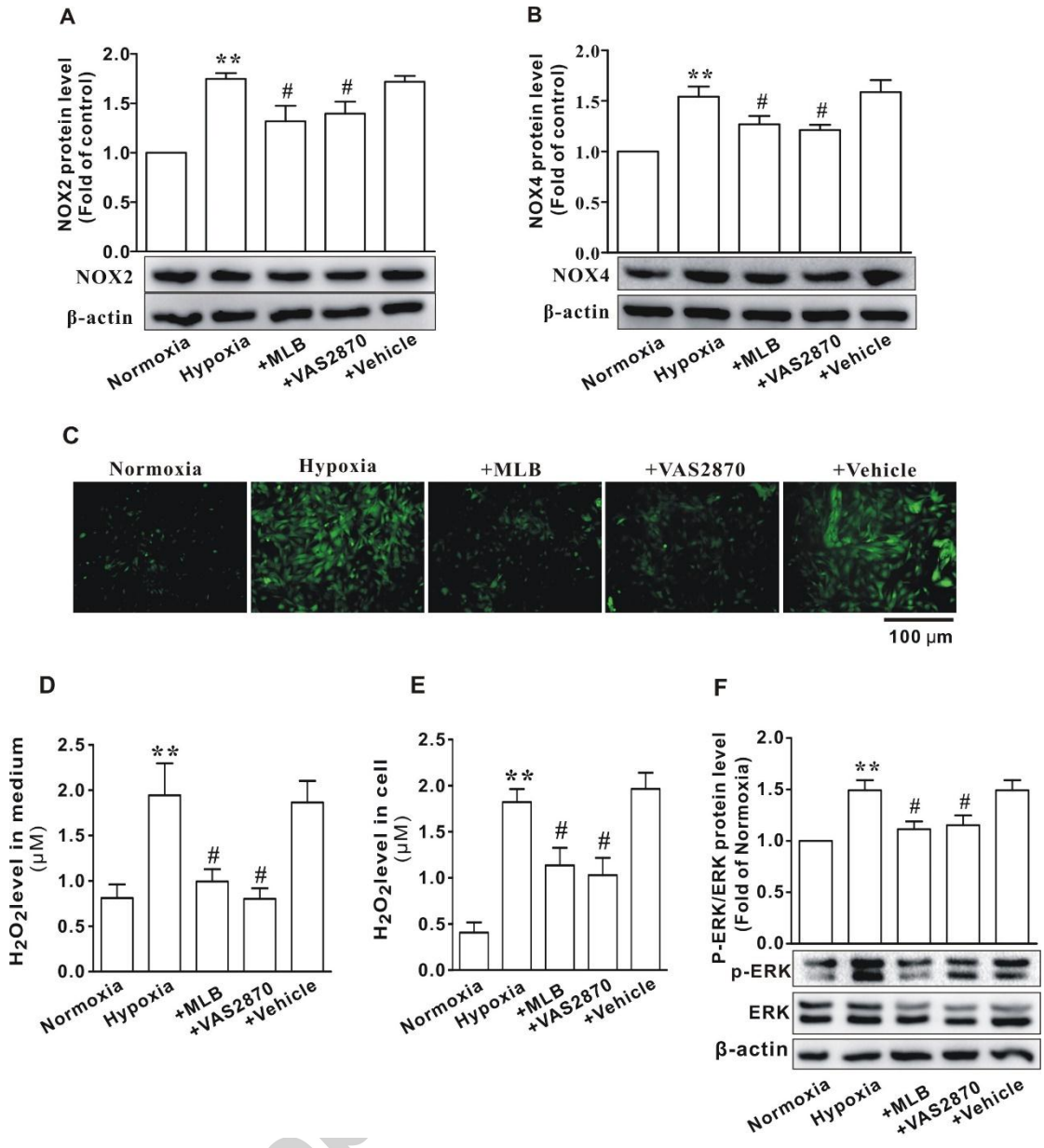

Figure 6